



Journal of Advanced Research in Applied Mechanics

Journal homepage:
<https://semarakilmujournal.com.my/index.php/aram/index>
ISSN: 2289-7895



3D Internal Stability Loss of Single-Walled CNT with Initial Defect in a Viscoelastic Body

Fatma Çoban Kayıkcı^{1,*}

¹ Faculty of Chemical and Metallurgical, Yıldız Technical University, 34349 Beşiktaş/İstanbul, Türkiye

ARTICLE INFO

Article history:

Received 29 October XXXX
Received in revised form 1 December XXXX
Accepted 9 December XXXX
Available online 10 December XXXX

Keywords:

Stability loss; carbon nanotubes;
viscoelasticity

ABSTRACT

In the current paper, the stability loss examination for a viscoelastic body reinforced single-walled carbon nanotube (SWCNT) having local curvature was achieved. The study is conducted by applying the piecewise-homogeneous body model and 3D linearized stability theory (TDLTS). It is assumed that the carbon nanotube (CNT) in this instance exhibits an initially localized imperfection that is insignificant and the growth of this imperfection in the course of time is investigated. The criterion for determining stability loss is defined as the infinite growth of the local curvature of the CNT. The critical time value and critical load value are determined according to this criterion. The fractional-exponential Rabotnov operator is used to characterize the properties of the composite material's viscoelasticity. Numerical results reveal the influence of key parameters, such as the thickness of the CNT and rheological properties, on the critical load and time values. Increasing the thickness of the CNT leads to a decrease in critical load, while rheological parameters significantly affect stability outcomes. These findings are critical for designing advanced engineering materials with enhanced stability and performance. This study provides a theoretical framework for understanding the mechanical behaviour of CNT-reinforced viscoelastic composites, offering insights into their practical applications. The results can guide the design of materials for specific uses in vibration control, energy storage etc. and contributing optimal performance under varying conditions. Furthermore, this research highlights the importance of viscoelasticity in defining the mechanical properties and stability constraints of composite materials with locally curved SWCNTs.

1. Introduction

The carbon nanotubes (CNTs) have been stimulated an abundance of possible uses owing to their high modulus of elasticity, high strength and their considerable properties as mechanical, optical and electronical after its discovery as mentioned by Baran *et al.*, [1]. These unique properties provide superiority in a wide range engineering applications such as biotechnology chemistry and defence industry. CNTs are named according to the layers they have. Single-layer tubes are called single-walled and those with more than one layer are called multi-walled CNTs by Malikan *et al.*, [2].

* Corresponding author.

E-mail address: fatmacbn@yildiz.edu.tr

<https://doi.org/10.37934/aram.137.1.160175>

Moreover, CNTs are one of the strongest materials known [3]. Due to the high cost and difficulty of conducting performance and control studies at the nanoscale, scientists and engineers focus on creating theoretical models as mentioned by Karličić *et al.*, [4].

According to Shi *et al.*, [5] there are various methods used for theoretical studies of the mechanical properties of CNTs, such as the molecular dynamics method, the molecular mechanics model, the finite element model and the classical continuum model. Despite the fact that molecular dynamics simulation is more practical than other approaches for analysis of nanomaterials because of their discrete structures, it is difficult to perform experiments at nano scale. For large-sized atomic systems, atomistic modelling is also computationally expensive. Thus, continuum modelling is crucial in the investigation of nanostructures' mechanical characteristics as described by Arefi *et al.*, [6]. The applicability of continuum mechanics in the investigation of nanostructures was discussed by Guz [7] and Duan *et al.*, [8]. The fracture of pre-cracked graphene layers (CNTs consist of graphene layers) with Peridynamics (PD) was modelled and is investigated with molecular simulation method by Liu *et al.*, [9].

According to many experimental observations, CNTs (most nanostructures) are mostly identified by a specific degree of fluctuation in their axial direction. The presence of a geometric imperfection exerts a substantial impact on the mechanical behaviour of carbon nanotubes. CNTs with initial defects have different mechanical behaviours than flat ones as told by Arefi *et al.*, [6]. The tubule curves as a result of the defects and CNTs have various tubule shapes including straight, wavy, helical and branched that have been observed and synthesized so far [10]. The nanotubes having curvature are widely utilized in a variety of engineering applications [2]. Looking at a brief review of studies on the analysis of the stability of elastic (or viscoelastic) body containing SWCNTs such as Arefi *et al.*, [6], it is investigated the stability of a CNT having light curvature under lateral loading in the context of Eringen's theory of nonlocal elasticity.

It is examined by Mehdipour *et al.*, [11] that the nonlinear force vibrational analysis of a placed curved SWCNT put in an elastic medium utilizing continuum mechanics and an elastic beam model. The paper by Berrabah *et al.*, [12], investigated the wave propagation in single-walled CNTs using nonlocal elasticity theory. Wang *et al.*, [13], the study focuses on analysing the phenomenon of elastic buckling in micro and nano-rods/tubes. This research is conducted using Eringen's nonlocal theory of elasticity and Timoshenko beam theory. It is analysed that the mechanical buckling behaviour of a single-walled carbon nanotube (SWCNT) integrated in an elastic medium [14]. Similar studies are also available for multi-walled carbon nanotubes (MWCNT) and generally MWCNTs are modelled as shell or column. For example, Ru [15], it was studied buckling of DWCNT subjected to axial load in elastic medium. In the paper by Yan *et al.*, [16], the behaviour of triple-walled CNTs (TWCNTs) was investigated with initial axial stress. Moreover, it is assumed that TWCNTs were consist of three elastic shells and van der Waals forces connected the shells. Thermal conductivity and stability of SWCNTs and MWCNTs are investigated by Jamil *et al.*, [17]. It is made that the viscoelastic evaluation of phenolic resin reinforced with CNTs [18]. The results obtained there show that CNT added to a phenolic resin matrix can significantly increase viscoelastic properties and change thermal stability.

Moreover, in study by Çoban Kayıkçı *et al.*, [19], stability analyses of CNTs placed in an elastic medium and with an initial primitive defect are performed separately for both two-layer and three-layer CNTs. Additionally, the stress analysis of two-layer CNT having curvature with an initial primitive defect was investigated by Çoban Kayıkçı *et al.*, [20]. Viscoelastic materials are speedily attained interest in damping applications and it is shown by Suhr *et al.*, [21] that with an increase of up to 1,400%, the material containing MWCNTs exhibits substantial viscoelastic behaviour.

In the paper by Malikan *et al.*, [2], the dynamic response of non-cylindrical curved viscoelastic monolayer CNTs is theoretically investigated. Here, the viscoelastic damping effect is evaluated

utilizing the Kelvin-Voigt viscoelastic model. The complicated mechanics of the viscoelastic CNT subjected to electrical load are investigated [22], utilizing the nonlocal continuum theory, the Kelvin-Voigt viscoelastic model and the Euler beam theory.

The microbuckling phenomenon of double-walled carbon nanotubes (DWCNT) placed within the polymer matrix was investigated [23]. The Three-Dimensional Linearized Theory of Stability of Deformable Bodies (TDLTSDB), which covers the model of a body that is homogeneous in different regions, was used to conduct the investigation. We review to a summary of TDLTSDB used in the present paper. This method is used in the stability problems for elastic or viscoelastic material. After 1950s, considerable contributions were provided to the development of TDLTS and it was used to solve a variety of stability loss issues with structural parts. In most cases, the TDLTS, which are the linearization method is employed to analyse instability issues of construction components by utilizing the equations and relations obtained from the exact nonlinear equations of deformable solid body mechanics as explained by Akbarov *et al.*, [24]. A comprehensive overview of the relevant investigation was carried out by Babich *et al.*, [25].

TDLTS was mostly applied in relation to the stability loss of components composed of time-independent materials. A method for stability analysis of structural members produced from time-dependent materials is proposed by Hoff *et al.*, [26]. That method was based on the increase of the initial defect in the structural elements with the flow of time under constant external static compression. Nevertheless, the aforesaid approach is not given in TDLTS. For the first time, in order to study of the stability loss in the longitudinal fibrous structure, Akbarov *et al.*, [27] proposed an approach. The gradual growth of the initially existing defects in the fibres is taken as the criterion for determining the critical load or critical time values, which are the parameters of the loss of stability [28]. In addition, the aforesaid approach was employed to investigate analyse the fibre buckling in a viscoelastic matrix [29], the symmetrical stability of a cylindrical material formed of viscoelastic composite was examined applying the 3D method. It was studied the theoretical limit of composites having hollow and locally curved fibres by Akbarov *et al.*, [30].

After all of these summarizations, it is seen that no study in the literature analyses stability loss of viscoelastic material containing the locally curved SWCNT employing the TDLTS. The current study is the initial effort to explore the stability analyses of SWCNT with local curvature in the viscoelastic material. Understanding the stability loss of single-walled carbon nanotubes (SWCNTs) embedded in viscoelastic matrices is a critical issue for the development of advanced composite materials. Despite significant progress in modelling CNTs, the impact of local curvature and viscoelasticity on stability has not been comprehensively explored. Existing studies often neglect the combined effects of localized imperfections and viscoelastic damping, leaving a gap in the theoretical understanding of these materials. By providing theoretical insights and numerical results, this research seeks to guide the design of CNT-reinforced composites with enhanced stability and performance. TDLTS is used within the context of the piecewise homogeneous body model in this paper and the SWCNT is modelled as a hollow cylinder.

2. Mathematical Formulation

In this problem, an infinite viscoelastic medium containing an infinitely long, low density and locally curved single-walled carbon nanotube (SWCNT) is considered. It is assumed that this body, which is shown in Figure 1, is affected by normal forces that uniformly distributed in the SWCNT direction at infinity. It will also be assumed that radii of the parts at right angles to the CNT surface do not change along the CNT.

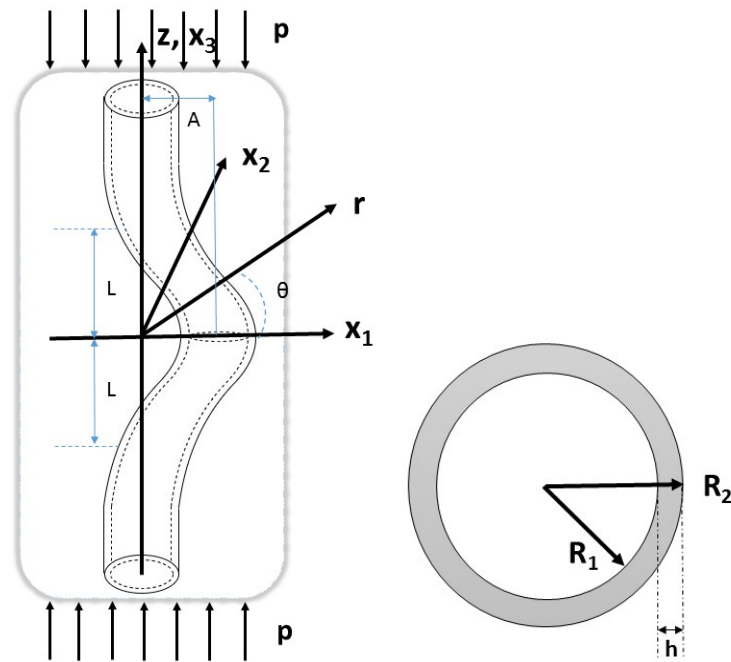


Fig. 1. The cross-sectional geometry of an infinitely viscoelastic body

As it can be seen in Figure 1, the $Ox_1x_2x_3$ Cartesian and $Or\theta z$ cylindrical coordinates systems with the starting point on the center line of the CNT are selected and these coordinates are assumed to be Lagrange coordinates. It will be considered that the viscoelastic body is under the influence of equally dispersed normal forces directed toward the CNT at a density of p (Ox_3) at infinity. It will also be assumed that the sections of the CNT perpendicular to the center line are circles with radii R_1 and R_2 and these radii do not change along the CNT. By assuming that the CNT and viscoelastic matrix are made up of different materials, the investigations will be made by applying the geometrical nonlinear three-dimensional exact equations of continuum mechanics. It is addressed the equation of centre line of CNT as:

$$x_1 = F(x_3) = \varepsilon \delta(x_3), \quad x_2 = 0 \quad (1)$$

The metric ($0 \leq \varepsilon < 1$) is used to quantify the magnitude of the bending amplitude of CNT. Additionally, $\delta(x_3)$ function displays the bending configuration of the CNT previous to loading. Indicated in Eq. (1), The central axis of the single-walled carbon nanotube (SWCNT), which has a primitive defect is situated inside the $x_2 = 0$ plane. Upon initialization, it is accepted that the central axis of the carbon nanotube (CNT) stays situated inside this plane. By using the equation denoted as Eq. (1) and considering the CNT-cross section condition, it can be derived the equation for S_2 , which represents the interface between the carbon nanotube (CNT) and the viscoelastic matrix, as described by Akbarov *et al.*, [31]. The equation is expressed as follows:

$$r(\theta, t_3) = \frac{\varepsilon \delta(t_3) (1 + \varepsilon^2 (\delta'(t_3))^2) \cos \theta}{1 + (\delta'(t_3))^2 \varepsilon^2 \cos^2 \theta} + \left\{ \frac{\varepsilon^2 (\delta(t_3))^2 (1 + \varepsilon^2 (\delta'(t_3))^2)^2 \cos \theta}{(1 + (\delta'(t_3))^2 \varepsilon^2 \cos^2 \theta)^2} + R^2 - (\delta(t_3))^2 \varepsilon^2 (1 + \varepsilon^2 (\delta'(t_3))^2) \right\}^{\frac{1}{2}},$$

$$x_3(\theta, t_3) = t_3 - \varepsilon \delta'(t_3) (r(\theta, t_3) - \varepsilon \delta(t_3)), \quad \delta'(t_3) = \frac{d\delta(t_3)}{dt_3} \quad (2)$$

Here t_3 is a parameter and $t_3 \in (-\infty, +\infty)$. The following equations are produced for the elements of the unit normal vector of the surface S_2 by using Eq. (2):

$$\begin{aligned} n_r &= r(\theta, t_3) \frac{\partial z(\theta, t_3)}{\partial t_3} [A(\theta, z)]^{-1} \quad n_\theta = \left[\frac{\partial z(\theta, t_3)}{\partial \theta} \frac{\partial r(\theta, t_3)}{\partial t_3} - \frac{\partial r(\theta, t_3)}{\partial \theta} \frac{\partial z(\theta, t_3)}{\partial t_3} \right] [A(\theta, z)]^{-1} \\ n_z &= r(\theta, t_3) \frac{\partial z(\theta, t_3)}{\partial t_3} [A(\theta, t_3)]^{-1} \end{aligned} \quad (3)$$

$A(\theta, t_3)$ as follows:

$$A(\theta, t_3) = \left[\left(r(\theta, t_3) \frac{\partial z(\theta, t_3)}{\partial t_3} \right)^2 + \left(r(\theta, t_3) \frac{\partial z(\theta, t_3)}{\partial t_3} \right)^2 + \left(\frac{\partial z(\theta, t_3)}{\partial \theta} \frac{\partial r(\theta, t_3)}{\partial t_3} - \frac{\partial z(\theta, t_3)}{\partial t_3} \frac{\partial r(\theta, t_3)}{\partial \theta} \right)^2 \right]^{1/2} \quad (4)$$

After that, the quantities related to the matrix material will be shown with Eq. (1) and the quantities related to the CNT with Eq. (2) superscripts. It is assumed that equilibrium equations, strain-displacement relations and constitutive equations are provided for each of the CNT and viscoelastic matrix materials:

$$\nabla_i [\sigma^{(k)in} (g_n^j + \nabla_n u^{(k)j})] = 0, \quad (5)$$

$$\begin{aligned} 2\varepsilon_{jm}^{(k)} &= \nabla_j u_m^{(k)} + \nabla_m u_j^{(k)} + \nabla_j u^{(k)n} \nabla_m u^{(k)n}, \\ \sigma_{(in)}^{(k)} &= \left(\lambda_0^{(k)} e^{(k)}(t) + \int_0^t \lambda^{(k)}(t - \tau) e^{(k)}(\tau) d\tau \right) \delta_i^n + 2 \left(\mu_0^{(k)} \varepsilon_{(in)}^{(k)}(t) + \int_0^t \mu^{(k)}(t - \tau) \varepsilon_{(in)}^{(k)}(\tau) d\tau \right), \quad e^{(k)} = \varepsilon_{11}^{(k)} + \varepsilon_{22}^{(k)} + \varepsilon_{33}^{(k)} \end{aligned} \quad (6)$$

The stress and strain tensors' respective physical components are specified by $\sigma_{(in)}^{(k)}$ and $\varepsilon_{(in)}^{(k)}$. Simultaneously, the S_2 surface—the interface between the CNT and the matrix—is assumed to have ideal contact conditions. These conditions are given as follows:

$$\sigma^{(2)in} (g_n^j + \nabla_n u^{(2)j}) \Big|_{S_1} n_j = 0, \quad (7)$$

$$\sigma^{(1)in} (g_n^j + \nabla_n u^{(1)j}) \Big|_{S_2} n_j = \sigma^{(2)in} (g_n^j + \nabla_n u^{(2)j}) \Big|_{S_2} n_j = 0, \quad u^{(1)j} \Big|_{S_2} = u^{(2)j} \Big|_{S_2}$$

$$\sigma_{zz}^{(1)} \xrightarrow{z \rightarrow \infty} p, \quad \sigma_{ij}^{(1)} \xrightarrow{r \rightarrow \infty} 0, \quad i, j \rightarrow r, \theta, z \quad (8)$$

Consequently, in the context of contact conditions Eq. (7) and Eq. (8), an analysis of Eq. (5) and Eq. (6) yields the general mathematical statement of the problem.

3. Solution Method

The aforementioned approach presents a boundary-value problem for a system of nonlinear partial differential equations. The problem is solved by using the border form perturbation approach as described by Akbarov *et al.*, [31]. In this approach, the desired variables are expressed as a series of the tiny parameter ε , incorporated in the equation representing CNT's central axis and indicates the extent of its curvature:

$$\left\{ \sigma_{(ij)}^{(m)}; \varepsilon_{(ij)}^{(m)}; u_{(i)}^{(m)} \right\} = \sum_{k=1}^{\infty} \varepsilon^k \left\{ \sigma_{(ij)}^{(m),k}; \varepsilon_{(ij)}^{(m),k}; u_{(i)}^{(m),k} \right\}, (ij) = rr; \theta\theta; x_3x_3; r\theta; rx_3; \theta x_3, (i) = r; \theta; x_3 \quad (9)$$

The expressions in Eq. (9) are written in the relevant equations and it is obtained the system of equations for each approximation. The coefficients (ε^m) in Eq. (9) is categorized based on the identical degrees of ε and expands to series (R, θ, t_3) and so for each approach, it is obtained the contact conditions provided at the $r = R_1$ and $r = R_2$ surfaces.

3.1 The Zeroth Approximation

For this approximation, Eq. (5) and Eq. (6) will be provided exactly. Considering that $n_r=1, n_\theta=0, n_z=0$, contact conditions Eq. (7) will be provided in $r = R_1$ and $r = R_2$. Furthermore, Eq. (8) conditions for the zeroth approximation takes the following form:

$$\sigma_{zz}^{(1),0} \xrightarrow{z \rightarrow \infty} p, \sigma_{zz}^{(1),0} \xrightarrow{r \rightarrow \infty} 0, (ij) \neq zz \quad (10)$$

By employing the zeroth approximation, one obtains nonlinear equations and contact conditions. The initial approximation (the zeroth) refers to the boundary value problem that needs to be analysed in order to determine the stability loss that occur when the CNT in the model is flat without curvature. In this instance, the nonlinear components in the equations generated for the zeroth approximation can be neglected since they will have very insignificant effects [31]. Therefore, assuming that the condition $\nabla_n u^{(k)j,0} \ll 1$ is provided, $g_n^j + \nabla_n u^{(k)j,0}$ terms will be replaced by the δ_n^j Kronecker symbols:

$$\nabla_i \sigma^{(k)ij,0} = 0, 2\varepsilon_{jm}^{(k),0} = \nabla_j u_i^{(k),0} + \nabla_m u_j^{(k),0} \quad (11)$$

$$\sigma_{(in)}^{(k),0} = \left(\lambda_0^{(k)} e^{(k)}(t) + \int_0^t \lambda^{(k)}(t - \tau) e^{(k)}(\tau) d\tau \right) \delta_i^n + 2 \left(\mu_0^{(k)} \varepsilon_{(in)}^{(k)}(t) + \int_0^t \mu^{(k)}(t - \tau) \varepsilon_{(in)}^{(k)}(\tau) d\tau \right)$$

$$e^{(k),0} = \varepsilon_{(rr)}^{(k),0} + \varepsilon_{(\theta\theta)}^{(k),0} + \varepsilon_{(zz)}^{(k),0}$$

$$\sigma_{(ij)}^{(2),0} \Big|_{r_q=R_1} = 0,$$

$$\sigma_{(ij)}^{(2),0} \Big|_{r_q=R_2} = \sigma_{(ij)}^{(1),0} \Big|_{r_q=R_2}, u_{(i)}^{(2),0} \Big|_{r_q=R_2} = u_{(i)}^{(1),0} \Big|_{r_q=R_2}; (ij) = rr, r\theta, rz (i) = r, \theta, z \quad (12)$$

Thus, the Eq. (11) and the contact conditions Eq. (12) required to determine the zeroth approximation has been obtained.

3.2 The First Approximation

When the procedure applied for the zeroth approximation is applied for the first approximation within the framework of the same assumptions, the relevant equations are obtained as follows:

$$\nabla_i \left[\sigma^{(k)ij,1} + \sigma^{(k)in,0} \nabla_n u^{(k)j,1} \right] = 0 \quad (13)$$

$$2\varepsilon_{ij}^{(k),1} = \nabla_j u_i^{(k),1} + \nabla_i u_j^{(k),1}$$

$$\sigma_{(in)}^{(1),0} = \left(\lambda_0^{(1)} e^{(1)}(t) + \int_0^t \lambda^{(1)}(t - \tau) e^{(1)}(\tau) d\tau \right) \delta_i^n + 2 \left(\mu_0^{(1)} \varepsilon_{(in)}^{(1)}(t) + \int_0^t \mu^{(1)}(t - \tau) \varepsilon_{(in)}^{(1)}(\tau) d\tau \right)$$

$$e^{(k),1} = \varepsilon_{(11)}^{(k),1} + \varepsilon_{(22)}^{(k),1} + \varepsilon_{(33)}^{(k),1} \quad (14)$$

The first approximation's contact conditions are given below:

$$[\sigma_{(i)r}]_{1,1}^{2,1} + f_1 \left[\frac{\partial \sigma_{(i)r}}{\partial r} \right]_{1,0}^{2,0} + \phi_1 \left[\frac{\partial \sigma_{(i)r}}{\partial z} \right]_{1,0}^{2,0} + \gamma_r [\sigma_{(i)r}]_{1,0}^{2,0} + \gamma_\theta [\sigma_{(i)\theta}]_{1,0}^{2,0} + \gamma_z [\sigma_{(i)z}]_{1,0}^{2,0} = 0 \quad (15)$$

$$[u_{(i)}]_{1,1}^{2,1} + f_1 \left[\frac{\partial u_{(i)}}{\partial r} \right]_{1,0}^{2,0} + \phi_1 \left[\frac{\partial u_{(i)}}{\partial z} \right]_{1,0}^{2,0} = 0$$

$$[\sigma_{(i)r}]_{1,1}^{2,1} + f_1 \left[\frac{\partial \sigma_{(i)r}}{\partial r} \right]_{1,0}^{2,0} + \phi_1 \left[\frac{\partial \sigma_{(i)r}}{\partial z} \right]_{1,0}^{2,0} + \gamma_r [\sigma_{(i)r}]_{1,0}^{2,0} + \gamma_\theta [\sigma_{(i)\theta}]_{1,0}^{2,0} + \gamma_z [\sigma_{(i)z}]_{1,0}^{2,0} = 0,$$

$$i = r, \theta, z$$

The first approximation is obtained by using the provided equations and contact conditions. The abbreviations used in Eq. (15) are as follows:

$$[\varphi]_{1,k}^{2,k} = \varphi^{(2),k} - \varphi^{(1),k}, \quad (16)$$

$$[\varphi]^{2,k} = \varphi^{(2),k}, f_1 = \delta(t_3) \cos\theta, \varphi_1 = -R \frac{d\delta(t_3)}{dt_3} \cos\theta$$

$$\gamma_r = \left(\frac{\delta(t_3)}{R} - \frac{d^2\delta(t_3)}{dt_3^2} R \right) \cos\theta, \gamma_\theta = \frac{\delta(t_3)}{R} \sin\theta, \gamma_z = -\frac{d\delta(t_3)}{dt_3} \cos\theta$$

The materials used to construct the SWCNT and the viscoelastic matrix are distinct. Matrix material and CNT Poisson rates are denoted as $\nu^{(1)}$ and $\nu^{(2)}$ whereas Young modulus of matrix material and CNT are denoted as $E^{(1)}$ and $E^{(2)}$, respectively. It is accepted that $\nu^{(2)} = \nu_0^{(1)}$ and $\nu^{(1)}|_{t=0} = \nu_0^{(1)}$ (t is time). In the zeroth approximation, the stresses caused by $\nu^{(2)} \neq \nu^{(1)}$ for $t > 0$ will not be taken into account because their order is $O(u^{(2)} - u^{(1)})$. Furthermore, as stated by Babich *et al.*, [32], do not significantly impact numerical outcomes. For the zeroth approximation, the following equations are found in this instance:

$$\varepsilon_{zz}^{(1),0} = \varepsilon_{zz}^{(2),0} = \frac{p}{E^{*(1)}}, \sigma_{zz}^{(1),0} = p, u_z^{(1),0} = u_z^{(2),0} = \frac{p}{E^{*(1)}} z, \quad (17)$$

$$u_\theta^{(1),0} = u_\theta^{(2),0} = 0, u_r^{(1),0} = -\nu^{*(1)} \varepsilon_{zz}^{(1),0} r, u_r^{(2),0} = -\nu^{(2)} \varepsilon_{zz}^{(2),0} r, \sigma_{rr}^{(1),0} = \sigma_{rr}^{(2),0} = \sigma_{\theta\theta}^{(1),0} = \sigma_{\theta\theta}^{(2),0} = 0$$

$$\sigma_{zz}^{(2),0} = p \frac{E^{(2)}}{E^{*(1)}}, \sigma_{\theta z}^{(1),0} = \sigma_{\theta z}^{(2),0} = \sigma_{rz}^{(1),0} = \sigma_{rz}^{(2),0} = \sigma_{r\theta}^{(1),0} = \sigma_{r\theta}^{(2),0} = 0$$

The following operators are represented by $E^{*(1)}$ and $\nu^{*(1)}$:

$$E^{*(1)} = E_0^{(1)} + \int_0^t E^{(1)}(t - \tau) d\tau, \nu^{*(1)} = \nu_0^{(1)} + \int_0^t \nu^{(1)}(t - \tau) d\tau \quad (18)$$

Here $\nu_0^{(1)}$ and $E_0^{(1)}$ are the instant Poisson ratio and Young's modulus [33]. Within the framework of the assumptions discussed above and considering the Eq. (17), when the Eq. (13) are written in

terms of the physical components of the relevant quantities in cylindrical coordinates, the following equations are obtained.

$$\begin{aligned} \frac{\partial \sigma_{rr}^{(k),1}}{\partial r} + \frac{1}{r} \frac{\partial \sigma_{r\theta}^{(k),1}}{\partial \theta} + \frac{\partial \sigma_{rz}^{(k),1}}{\partial z} + \frac{1}{r} \left(\sigma_{rr}^{(k),1} - \sigma_{\theta\theta}^{(k),1} \right) + \sigma_{zz}^{(k),0} \frac{\partial^2 u_r^{(k),1}}{\partial z^2} &= 0, \\ \frac{\partial \sigma_{r\theta}^{(k),1}}{\partial r} + \frac{1}{r} \frac{\partial \sigma_{\theta\theta}^{(k),1}}{\partial \theta} + \frac{\partial \sigma_{\theta z}^{(k),1}}{\partial z} + \frac{2}{r} \sigma_{r\theta}^{(k),1} + \sigma_{zz}^{(k),0} \frac{\partial^2 u_\theta^{(k),1}}{\partial z^2} &= 0, \\ \frac{\partial \sigma_{rz}^{(k),1}}{\partial r} + \frac{1}{r} \frac{\partial \sigma_{\theta z}^{(k),1}}{\partial \theta} + \frac{\partial \sigma_{zz}^{(k),1}}{\partial z} + \frac{1}{r} \sigma_{rz}^{(k),1} + \sigma_{zz}^{(k),0} \frac{\partial^2 u_z^{(k),1}}{\partial z^2} &= 0 \end{aligned} \quad (19)$$

These equations are observed to be in accordance with the three-dimensional linearized stability equations. Guz [34] when checked directly. Moreover, the geometrical relations as following:

$$\begin{aligned} \varepsilon_{rr}^{(k),1} = \frac{\partial u_r^{(k),1}}{\partial r}, \varepsilon_{\theta\theta}^{(k),1} = \frac{1}{r} \frac{\partial u_\theta^{(k),1}}{\partial \theta} + \frac{u_r^{(k),1}}{r}, \varepsilon_{zr}^{(k),1} = \frac{1}{2} \left(\frac{\partial u_z^{(k),1}}{\partial r} + \frac{\partial u_r^{(k),1}}{\partial z} \right) \\ \varepsilon_{zz}^{(k),1} = \frac{\partial u_z^{(k),1}}{\partial z}, \varepsilon_{r\theta}^{(k),1} = \frac{1}{2} \left(\frac{1}{r} \frac{\partial u_r^{(k),1}}{\partial \theta} + \frac{\partial u_\theta^{(k),1}}{\partial r} - \frac{u_\theta^{(k),1}}{r} \right), \varepsilon_{\theta z}^{(k),1} = \frac{1}{2} \left(\frac{\partial u_\theta^{(k),1}}{\partial z} + \frac{1}{r} \frac{\partial u_z^{(k),1}}{\partial \theta} \right) \end{aligned} \quad (20)$$

The explicit form of the equation of the centreline of CNT given by Eq. (1) is as follows:

$$x_1 = A \exp \left(- \left(\frac{x_3}{L} \right)^2 \right) \cos \left(m \frac{x_3}{L} \right) = \varepsilon L \exp \left(- \left(\frac{x_3}{L} \right)^2 \right) \cos \left(m \frac{x_3}{L} \right) = \varepsilon \delta(x_3) \quad (21)$$

The ε in Eq. (21) is chosen as $\varepsilon = \frac{A}{L}$ with the $L > A$ acceptance. The contact conditions Eq. (15) for the initial approximation are as follows:

$$\begin{aligned} \left(\sigma_{rr}^{(1),1} - \sigma_{rr}^{(2),1} \right) \Big|_{(R_2, \theta, t_3)} &= 0, \left(\sigma_{r\theta}^{(1),1} - \sigma_{r\theta}^{(2),1} \right) \Big|_{(R_2, \theta, t_3)} &= 0, \\ \left(\sigma_{rz}^{(1),1} - \sigma_{rz}^{(2),1} \right) \Big|_{(R_2, \theta, t_3)} &= \left(\sigma_{zz}^{(1),0} - \sigma_{zz}^{(2),0} \right) \frac{d\delta(t_3)}{dt_3} \cos\theta \\ \left(u_r^{(1),1} - u_r^{(2),1} \right) \Big|_{(R_2, \theta, t_3)} &= 0, \left(u_\theta^{(1),1} - u_\theta^{(2),1} \right) \Big|_{(R_2, \theta, t_3)} &= 0, \\ \left(u_z^{(1),1} - u_z^{(2),1} \right) \Big|_{(R_2, \theta, t_3)} &= 0, \sigma_{rr}^{(2),1} \Big|_{(R_1, \theta, t_3)} &= 0, \\ \sigma_{r\theta}^{(2),1} \Big|_{(R_1, \theta, t_3)} &= 0, \sigma_{rz}^{(2),1} \Big|_{(R_1, \theta, t_3)} &= \sigma_{zz}^{(2),0} \frac{d\delta(t_3)}{dt_3} \cos\theta \end{aligned} \quad (22)$$

For the solution of these equations, the following representation will be used by taking the Eq. (19) into consideration [34]:

$$\begin{aligned} u_r^{(k)} &= \frac{1}{r} \frac{\partial}{\partial \theta} \psi^{(k)} - \frac{\partial^2}{\partial r \partial z} \chi^{(k)}, u_\theta^{(k)} = -\frac{\partial}{\partial r} \psi^{(k)} - \frac{1}{r} \frac{\partial^2}{\partial \theta \partial z} \chi^{(k)}, \\ u_z^{(k)} &= \left(\lambda^{(k)} + \mu^{(k)} \right)^{-1} \left(\left(\lambda^{(k)} + 2\mu^{(k)} \right) \Delta_1 + \left(\mu^{(k)} + \sigma_{zz}^{(k),0} \right) \frac{\partial^2}{\partial z^2} \right) \chi^{(k)}, \\ \Delta_1 &= \frac{\partial^2}{\partial r^2} + \frac{1}{r} \frac{\partial}{\partial r} + \frac{1}{r^2} \frac{\partial^2}{\partial \theta^2}. \end{aligned} \quad (23)$$

The $\psi^{(k)}$, $\chi^{(k)}$ functions provide the following equations:

$$\left(\Delta_1^{(k)} + \left(\xi_1^{(k)} \right)^2 \frac{\partial^2}{\partial z^2} \right) \psi^{(k)} = 0, \left(\Delta_1^{(k)} + \left(\xi_2^{(k)} \right)^2 \frac{\partial^2}{\partial z^2} \right) \left(\Delta_1^{(k)} + \left(\xi_3^{(k)} \right)^2 \frac{\partial^2}{\partial z^2} \right) \chi^{(k)} = 0 \quad (24)$$

$\xi_i^{(k)}$ ($k=1,2 ; i=1,2,3$) in Eq. (24) is defined as follows:

$$\xi_1^{(k)} = \sqrt{\frac{\mu^{(k)} + \sigma_{zz}^{(k),0}}{\mu^{(k)}}}, \xi_2^{(k)} = \sqrt{\frac{\mu^{(k)} + \sigma_{zz}^{(k),0}}{\mu^{(k)}}}, \xi_3^{(k)} = \sqrt{\frac{\lambda^{(k)} + 2\mu^{(k)} + \sigma_{zz}^{(k),0}}{\lambda^{(k)} + 2\mu^{(k)}}} \quad (25)$$

The above equations are subjected to the exponential Fourier transform by $z = \frac{x_3}{L}$ in order to resolve the boundary value problem associated with the first approximation:

$$\bar{V}(r, \theta, z) = \int_{-\infty}^{\infty} V(r, \theta, z) e^{-ix_3z} dx_3 \quad (26)$$

The following equations result from solving Eq. (24) differential equations taking into account the equilibrium equations and contact conditions after the Fourier transformation is applied.

$$\begin{aligned} \bar{\psi}_1^{(1),1} &= \bar{\Lambda}_1^{(1)}(s) K_1(\mathcal{E}_1^{(1)}) \sin \theta, \\ \bar{\chi}_1^{(1),1} &= i \left[\bar{\Lambda}_2^{(1)}(s) K_1(\mathcal{E}_2^{(1)}) + \bar{\Lambda}_3^{(1)}(s) K_1(\mathcal{E}_3^{(1)}) \right] \cos \theta \\ \bar{\chi}_2^{(2),1} &= \left[\bar{\Lambda}_{11}^{(2)}(s) I_1(\mathcal{E}_1^{(2)}) + \bar{\Lambda}_{12}^{(2)}(s) K_1(\mathcal{E}_1^{(2)}) \right] \sin \theta, \\ \bar{\beta}_2^{(2),1} &= i \left[\bar{\Lambda}_{21}^{(2)}(s) I_1(\mathcal{E}_2^{(2)}) + \bar{\Lambda}_{22}^{(2)}(s) K_1(\mathcal{E}_2^{(2)}) + \bar{\Lambda}_{31}^{(2)}(s) I_1(\mathcal{E}_3^{(2)}) + \bar{\Lambda}_{32}^{(2)}(s) K_1(\mathcal{E}_3^{(2)}) \right] \cos \theta \end{aligned} \quad (27)$$

In Eq. (27), $\mathcal{E}_j^{(q)} = \xi_j^{(q)} s \frac{r}{L}$, ($j = 1,2,3; q = 1,2$), $I_n(x)$ is the Bessel functions and $K_n(x)$ is the Macdonald functions. When the functions in Eq. (23) are written in related equations, a system of linear equations consisting of 15 equations with 15 variables is created. By solving this linear equation system, the unknowns are determined. The values of the stresses and displacement after applying Fourier transforms are obtained using the unknowns. The inverse Fourier transform is then used to obtain real values. The boundary value problem for the first approximation has been concluded in this manner. The further iterations, starting with the second approximation, do not have any impact on the final outcomes, as demonstrated by Kosker [33]. Therefore, the first approximation is sufficient for obtaining the numerical outcomes.

4. Numerical Results and Discussion

In the numerical results, it is utilized the parameters $R_2 = R$ for the outer radius, R_1 for the inner radius and h for the thickness of the CNT. $\frac{R}{L}$ and $\frac{h}{L}$ are defined as dimensionless parameters. Considering that the material examined is CNT, the value range determined for the relevant parameters is as follows [23].

$$400 \leq \frac{E^{(2)}}{E_0^{(1)}} \leq 1000, 0.15 \leq \frac{h}{L} \leq 0.35, 0.25 \leq \frac{R}{L} \leq 1. \quad (28)$$

$E_0^{(1)}$ is the viscoelastic matrix's initial value. Rabotnov operators has been used to describe the constitutive relations for the viscoelastic matrix [35].

$$\begin{aligned}
 E^{*(1)} &= E_0^{(1)} [1 - \omega_0 R_{\alpha'}^* (-\omega_0 - \omega_\infty)] \\
 \nu^{*(1)} &= \nu_0^{(1)} \left[1 + \frac{1 - 2\nu_0^{(1)}}{2\nu_0^{(1)}} \omega_0 R_{\alpha'}^* (-\omega_0 - \omega_\infty) \right] \\
 \lambda^{*(1)} &= \lambda_0^{(1)} \left\{ 1 + \frac{1 - 2\nu_0^{(1)}}{2\nu_0^{(1)}(1 + \nu_0^{(1)})} \omega_0 R_{\alpha'}^* \left[-\frac{3}{2(1 + \nu_0^{(1)})} \omega_0 - \omega_\infty \right] \right\} \\
 \mu^{*(1)} &= \mu_0^{(1)} \left\{ 1 - \frac{3\omega_0}{2\nu_0^{(1)}(1 + \nu_0^{(1)})} R_{\alpha'}^* \left[-\frac{3}{2(1 + \nu_0^{(1)})} \omega_0 - \omega_\infty \right] \right\}
 \end{aligned} \tag{29}$$

$E_0^{(1)}$ and $\nu_0^{(1)}$ shown in Eq. (29) are instantaneous value of Young's modulus and instantaneous value of Poisson coefficient, respectively. Furthermore, $\lambda_0^{(1)}$ and $\mu_0^{(1)}$ precisely determine the instantaneous values of Lamé's constants. The matrix material's rheological properties consist of α' , ω_0 , ω_∞ and $R_{\alpha'}^*$, which represents the fractional-exponential Rabotnov operator [35]. The reason why Rabotnov operator are preferred in this study is that it allows the first parts of the experimental and theoretically created creep and relaxation graphs to be examined with high precision. Furthermore, the operator takes into account the asymptotic values of the identified graphs with high precision when the time goes to infinity. It also ensures practicality in mathematical operations. In addition, the dimensionless rheological parameter, denoted as ω and the dimensionless time, denoted as t' , respectively and expressed as $\omega = \omega_\infty/\omega_0$ and $t' = \omega_0^{1/(1+\alpha')}t$. Furthermore, it is supposed that $\nu_0^{(1)} = \nu^{(2)} = 0.3$ and $\epsilon = p/E_0^{(1)}$. According to Akbarov *et al.*, [29], the following inequalities must be satisfied by the external compressive force p while examining the stability loss problems of viscoelastic materials:

$$\epsilon_{cr,\infty} \left(= \frac{p_{cr,\infty}}{E_0^{(1)}} \right) \leq \epsilon \left(= \frac{p}{E_0^{(1)}} \right) \leq \epsilon_{cr,0} \left(= \frac{p_{cr,0}}{E_0^{(1)}} \right) \tag{30}$$

where $\epsilon_{cr,0}$ is the critical load obtained at $t' = 0$ and $\epsilon_{cr,\infty}$ is the critical load obtained at $t' = \infty$.

Table 1 shows the values of $\epsilon_{cr}|_{t'=0} = \epsilon_{cr,0}$ for $\frac{E^{(2)}}{E_0^{(1)}}$ the ratio of modulus of elasticity, $\frac{R}{L}$ the outer radius of SWCNT and the values of $\epsilon_{cr}|_{t'=\infty} = \epsilon_{cr,\infty}$ acquired for numerous ω and the results are presented for $\alpha = -0.5$. Besides, when $\frac{E^{(2)}}{E_0^{(1)}}$ values increase, the value of $\epsilon_{cr,0}$ decrease monotonically. Also, as the increase of thickness of CNT, $\epsilon_{cr,0}$ declines. Furthermore, the $\epsilon_{cr,\infty}$ values increase when the ω rheological parameter rises, whereas there is no relationship between the critical load and the α parameter.

Table 1

For diverse values of $E^{(2)}/E_0^{(1)}$ and h/L , $\epsilon_{cr,\infty}$ values at $t' = \infty$ and $\epsilon_{cr,0}$ values at $t' = 0$ ($\alpha = -0.5, R/L = 0.5$)

$E^{(2)}/E_0^{(1)}$	h/L	$\epsilon_{cr,0}$	$(\alpha = -0.5) \epsilon_{cr}$			
			$\omega = 0.5$	$\omega = 1.0$	$\omega = 2.0$	$\omega = 3.0$
500	0.35	0.0544	0.0306	0.0375	0.0439	0.0466
	0.25	0.0648	0.0363	0.0449	0.0524	0.0557
	0.15	0.0846	0.0480	0.0592	0.0690	0.0724
800	0.35	0.0422	0.0232	0.0290	0.0338	0.0362
	0.25	0.0507	0.0281	0.0349	0.0408	0.0436
	0.15	0.0667	0.0372	0.0463	0.0539	0.0577
1000	0.35	0.0375	0.0208	0.0257	0.0307	0.0322
	0.25	0.0449	0.0249	0.0309	0.0364	0.0385
	0.15	0.0592	0.0332	0.0413	0.0480	0.0509

Table 2 shows that the critical load is unaffected by the outer radius of CNT. parameter does not have an effect on the critical load.

It is seen in Table 2 that outer radius of CNT has no effect on critical load. This means that when the thickness of the CNT is constant, the space in the CNT (indicated by the R_1 in Figure 1) is not significant.

Table 2

For diverse values of $E^{(2)}/E_0^{(1)}$ and R/L , $\epsilon_{cr,0}$ values at $t' = 0$ ($h/L = 0.35$)

$E^{(2)}/E_0^{(1)}$	R/L									
	1	0.8	0.7	0.5	0.35	0.3	0.28	0.27	0.26	0.255
500	0.0648	0.0648	0.0649	0.0648	0.0649	0.0649	0.0649	0.0652	0.0648	0.0648
800	0.0508	0.0506	0.0509	0.0507	0.0509	0.0506	0.0507	0.0507	0.0506	0.0508
1000	0.0449	0.0449	0.0449	0.0449	0.0454	0.0450	0.0450	0.0450	0.0449	0.0450

As can be seen in Table 3, the critical time t'_{cr} is calculated for various values of the parameters $\frac{E^{(2)}}{E_0^{(1)}}$, α and $\epsilon_{cr,\infty}$. The findings are provided for the value of $\omega = 0.5$. The ϵ_{cr} values are chosen from the range between $\epsilon_{cr,0}$ and $\epsilon_{cr,\infty}$ as specified in Table 1. As the specified values converge to $\epsilon_{cr,0}$, the critical time $t'_{cr} \rightarrow 0$ and when the values converge to $\epsilon_{cr,\infty}$, the critical time $t'_{cr} \rightarrow \infty$ as expected. Moreover, Table 3 reveals a negative correlation between t'_{cr} values and the absolute value of the rheological parameter α .

Table 3
 For diverse values of α and $E^{(2)}/E_0^{(1)}$,
 t'_{cr} values ($\omega=0.5, h/L=0.25, R/L=0.5$)

$E^{(2)}/E_0^{(1)}$	ϵ_{cr}	t'_{cr}		
		$\alpha=-0.3$	$\alpha=-0.5$	$\alpha=-0.7$
500	0.0479	0.0930	0.0450	0.0093
	0.0492	0.0588	0.0250	0.0034
	0.0505	0.0349	0.0122	0.0011
	0.0518	0.0173	0.0045	0.0002
	0.0531	0.0055	0.0012	0.0000
800	0.0372	0.0905	0.0456	0.0092
	0.0382	0.0592	0.0254	0.0034
	0.0392	0.0357	0.0124	0.0012
	0.0402	0.0183	0.0048	0.0007
	0.0412	0.0061	0.0011	0.0001
1000	0.0331	0.0852	0.0421	0.0080
	0.0340	0.0550	0.0228	0.0029
	0.0349	0.0324	0.0108	0.0009
	0.0358	0.0156	0.0040	0.0001
	0.0367	0.0044	0.0006	0.0000

It is demonstrated in Figure 2 that when rheological parameter values ω increases, t'_{cr} values rise.

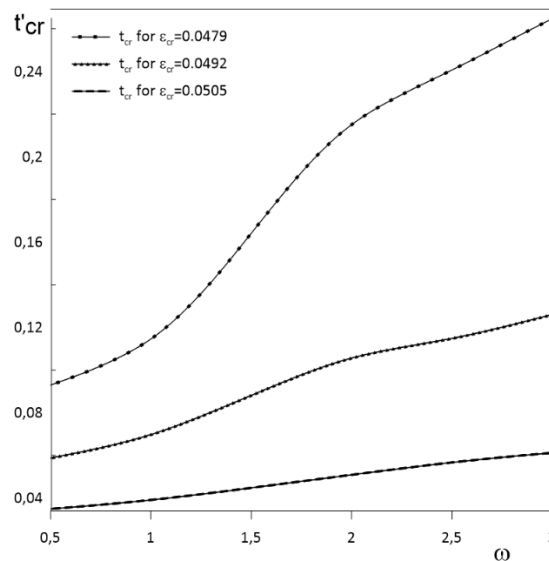


Fig. 2. For diverse values of $E^{(2)}/E_0^{(1)}$ and ω ,
 t'_{cr} values ($\alpha=-0.3, R/L=0.5, h/L=0.35$)

Furthermore, Table 4 demonstrates a correlation between a drop in the values of t'_{cr} and a reduction in the ratio $\frac{E^{(2)}}{E_0^{(1)}}$. Additionally, ϵ_{cr} value decreases as $\frac{E^{(2)}}{E_0^{(1)}}$ increases. t'_{cr} values decline when this circumstance is considered in relation to critical time values.

Table 4

For diverse values of $E^{(2)}/E_0^{(1)}$, t'_{cr}
 values ($\alpha=-0.3$, $\omega=1$, $R/L=0.5$, $h/L=0.35$)

ϵ_{cr}	$E^{(2)}/E_0^{(1)}$	t'_{cr}
0.0370	800	0.12540
	850	0.06920
	900	0.03450
	950	0.01360
	1000	0.00200
	1050	0.00004

When the value of R_1 is 0, the subject turns a stability loss problem in a medium that is both endlessly viscoelastic and includes an infinitely long fibre with locally curved. Under these circumstances, the value of the critical load is determined as $\epsilon_{cr} = -0.0982$ for $\omega = 2$, $\alpha = -0.5$, $\frac{E^{(2)}}{E_0^{(1)}} = 50$. It closely approximates the $\epsilon_{cr} = -0.0985$ value found by Guz [34], which used the same characteristics to study the stability loss of a viscoelastic body comprising fibres that have local curvature. Our Fortran-based approach, algorithms and the accuracy of the methodology are clearly demonstrated by this. Furthermore, the augmentation (reduction) of the rheological parameter ω ($|\alpha|$) leads to an increase in the critical time, as stated by Akbarov *et al.*, [36]. This outcome is congruent with the findings of this investigation.

The theoretical approach utilized in this study, specifically the Three-Dimensional Linearized Theory of Stability (TDLTS), offers several advantages over other modelling techniques or experimental methods. One of the key advantages is its ability to provide detailed insights into the stability loss of viscoelastic materials under varying conditions without the need for complex and costly experimental setups. This method allows for the precise analysis of critical parameters, such as critical load and time values, which are difficult to measure experimentally at the nanoscale. Furthermore, the theoretical framework is adaptable, enabling the investigation of a wide range of material properties and configurations, including those with initial defects or complex geometries.

However, the theoretical approach also has limitations. It relies heavily on simplifying assumptions, such as ideal material behaviour and uniform distribution of forces, which may not fully capture the complexities of real-world scenarios. Additionally, the accuracy of the results is contingent upon the validity of the input parameters and the mathematical models used. Compared to experimental methods, theoretical models may lack the ability to account for unforeseen environmental factors or material imperfections that could significantly influence the outcomes. Similarly, while molecular dynamics simulations offer atomistic-level precision, they are computationally expensive and limited in scale, making the TDLTS approach a more feasible alternative for large-scale studies.

By highlighting these advantages and limitations, this study aims to provide a balanced perspective on the applicability and reliability of the theoretical approach, offering a foundation for future research to build upon and complement with experimental validation.

5. Conclusion

Numerous aspects relating to the stability loss of the composite material created by adding single-walled and local curvature CNT to a viscoelastic matrix were given numerical findings. SWCNT is

considered as a continuous material and modelled as a hollow cylinder with infinite length. Continuum mechanics principles are utilised for the solution.

Moreover, it is assumed that there is a defect in the modelled nanotube that may have occurred during the processes. Current calculations were made via TDLTS. The fact that the initially accepted defect, in other words the local curvature, gradually grows and goes to infinity is recognized as the criteria for stability loss and the load value at this specific point is designated as the critical load. All of the results are obtained from zero and the first approach. Since the 2nd and subsequent approaches do not have a significant effect on the results, it is sufficient to restrict to the 1st approach.

Stability analysis of a single-walled CNT with an initial primitive defect embedded in a viscoelastic medium using a 3D approximate analytical method has been described for the first time in the literature using TDLTS.

In the related problem, the modulus of elasticity for SWCNT is $E^{(2)}$ and the starting value of the viscoelastic matrix's modulus of elasticity is $E_0^{(1)}$. The ratio of $\frac{E^{(2)}}{E_0^{(1)}}$ is included in the computations as 1000, 800 and 500. When examining the impact of this ratio on the related parameters, it becomes evident that as the ratio $\frac{E^{(2)}}{E_0^{(1)}}$ grows, the critical load values decline. Critical time values, on the contrary, increase with increasing $\frac{E^{(2)}}{E_0^{(1)}}$. Upon examining the impacts of the rheological factors ω and α on the findings, it is determined that the critical load values rise as the ω parameter increases. However, the α parameter does not have impact on the critical load. Furthermore, there is an inverse relationship between the rheological parameter α and the critical time, the critical time values decrease as the absolute value of rheological parameters α increase. However, there is a direct ratio between the rheological parameter α and the critical time and as ω increases, the critical time values also increase.

Based on these findings, properties such as the radius and thickness of the reinforcing SWCNT can be determined by the desired properties of the composite material to be produced. In addition, the parameters of the viscoelastic medium can be selected in the same way. Thus, the cost of the planned experiments is reduced. Obtaining theoretical results for carbon nanotubes, which have an essential role in damping viscoelastic materials, will be pioneering and guiding in the transformation of processes into practice.

The findings of this study provide valuable insights for the design and optimization of viscoelastic reinforced carbon nanotube (CNT) composites. Specifically, such materials can be utilized in damping applications where energy dissipation is crucial, such as in aerospace and automotive components. Moreover, the ability to predict critical load and time values offers significant advantages in designing lightweight and high-strength structural materials for use in advanced engineering fields. For instance, the critical load data can guide the development of composite materials used in vibration control systems, while the time-dependent viscoelastic properties can enhance the durability and stability of flexible electronics and biomedical devices.

To advance the understanding and application of viscoelastic reinforced carbon nanotube (CNT) composites, several avenues for future research can be explored. First, investigating the effects of different nanostructure geometries, such as helical or branched CNTs, could provide valuable insights into the mechanical behaviour and stability characteristics of these materials. Second, employing alternative viscoelastic models, including fractional derivative models or advanced constitutive equations, could enhance the accuracy and applicability of theoretical predictions. Third, incorporating multiphysics phenomena, such as thermal effects, electrical loading or fluid-structure

interactions, into the analysis would allow for a more comprehensive understanding of CNT composites under realistic operating conditions. These research directions not only extend the scope of current findings but also provide a roadmap for integrating experimental and theoretical efforts to address complex challenges in the field of nanomaterial engineering.

Acknowledgement

This research was not funded by any grant.

References

- [1] Baran, Jakub D., Wojciech Kołodziejczyk, Peter Larsson, Rajeev Ahuja and J. Andreas Larsson. "On the stability of single-walled carbon nanotubes and their binding strengths." *Theoretical Chemistry Accounts* 131 (2012): 1-8. <https://doi.org/10.1007/s00214-012-1270-3>
- [2] Malikan, Mohammad, Van Bac Nguyen, Rossana Dimitri and Francesco Tornabene. "Dynamic modeling of non-cylindrical curved viscoelastic single-walled carbon nanotubes based on the second gradient theory." *Materials Research Express* 6, no. 7 (2019): 075041. <https://doi.org/10.1088/2053-1591/ab15ff>
- [3] Jena, Subrat Kumar, S. Chakraverty, Mohammad Malikan and Francesco Tornabene. "Stability analysis of single-walled carbon nanotubes embedded in winkler foundation placed in a thermal environment considering the surface effect using a new refined beam theory." *Mechanics Based Design of Structures and Machines* 49, no. 4 (2021): 581-595. <https://doi.org/10.1080/15397734.2019.1698437>
- [4] Karličić, Danilo, Predrag Kozić, Ratko Pavlović and Nikola Nešić. "Dynamic stability of single-walled carbon nanotube embedded in a viscoelastic medium under the influence of the axially harmonic load." *Composite Structures* 162 (2017): 227-243. <https://doi.org/10.1016/j.compstruct.2016.12.003>
- [5] Shi, Jin-Xing, Toshiaki Natsuki, Xiao-Wen Lei and Qing-Qing Ni. "Buckling instability of carbon nanotube atomic force microscope probe clamped in an elastic medium." *Journal of Nanotechnology in Engineering and Medicine* 3, no. 2 (2012): 020903. <https://doi.org/10.1115/1.4007215>
- [6] Arefi, Azam and Hassan Nahvi. "Stability analysis of an embedded single-walled carbon nanotube with small initial curvature based on nonlocal theory." *Mechanics of Advanced Materials and Structures* 24, no. 11 (2017): 962-970. <https://doi.org/10.1080/15376494.2016.1196800>
- [7] Guz, Igor. "Continuum solid mechanics at nano-scale: How small can it go?." *Journal of Nanomaterials & Molecular Nanotechnology* 1, no. 1 (2012).
- [8] Duan, H. L., Jianxiang Wang and Bhushan Lal Karihaloo. "Theory of elasticity at the nanoscale." *Advances in applied mechanics* 42 (2009): 1-68. [https://doi.org/10.1016/S0065-2156\(08\)00001-X](https://doi.org/10.1016/S0065-2156(08)00001-X)
- [9] Liu, Xuefeng, Zhiwu Bie, Jinbao Wang, Ligang Sun, Meiling Tian, Erkan Oterkus and Xiaoqiao He. "Investigation on fracture of pre-cracked single-layer graphene sheets." *Computational Materials Science* 159 (2019): 365-375. <https://doi.org/10.1016/j.commatsci.2018.12.014>
- [10] Zhang, Mei and Jian Li. "Carbon nanotube in different shapes." *Materials today* 12, no. 6 (2009): 12-18. [https://doi.org/10.1016/S1369-7021\(09\)70176-2](https://doi.org/10.1016/S1369-7021(09)70176-2)
- [11] Mehdipour, Iman, Amin Barari, Amin Kimiaefar and G. Domairry. "Vibrational analysis of curved single-walled carbon nanotube on a Pasternak elastic foundation." *Advances in Engineering Software* 48 (2012): 1-5. <https://doi.org/10.1016/j.advengsoft.2012.01.004>
- [12] Berrabah, H. M., N. Z. Sekrane and B. E. Adda. "Comparative study of sound wave propagation in single-walled carbon nanotubes using nonlocal elasticity for two materials (Al) and (Ni)." *Journal of Advanced Research in Fluid Mechanics and Thermal Sciences* 18, no. 1 (2016).
- [13] Wang, C. M., Y. Y. Zhang, Sai Sudha Ramesh and S. Kitipornchai. "Buckling analysis of micro-and nano-rods/tubes based on nonlocal Timoshenko beam theory." *Journal of Physics D: Applied Physics* 39, no. 17 (2006): 3904. <https://doi.org/10.1088/0022-3727/39/17/029>
- [14] Selmoune, Belkacem, Abdelwahed Semmah, Mohammed L. Bouchareb, Fouad Bourada, Abdelouahed Tounsi and Mohammed A. Al-Osta. "Stability analysis of integrated SWCNT reposed on Kerr medium under longitudinal magnetic field effect Via an NL-FSDT." *Advances in materials Research* 12, no. 3 (2023): 243-261.
- [15] Ru, C. Q. "Axially compressed buckling of a doublewalled carbon nanotube embedded in an elastic medium." *Journal of the Mechanics and Physics of Solids* 49, no. 6 (2001): 1265-1279. [https://doi.org/10.1016/S0022-5096\(00\)00079-X](https://doi.org/10.1016/S0022-5096(00)00079-X)
- [16] Yan, Y., W. Q. Wang and L. X. Zhang. "Nonlocal effect on axially compressed buckling of triple-walled carbon nanotubes under temperature field." *Applied Mathematical Modelling* 34, no. 11 (2010): 3422-3429. <https://doi.org/10.1016/j.apm.2010.02.031>

- [17] Jamil, Muhammad Mahmud, Nor Azwadi Che Sidik, Umar Sanusi Umar, Muhammad Tukur Hamisu and Aisha Sa'ad. "Carbon nanotube for solar energy applications: A review." *Journal of Advanced Research in Fluid Mechanics and Thermal Sciences* 56, no. 2 (2019): 233-247.
- [18] Botelho, Edson Cocchieri, Michelle Leali Costa, Carlos Isidoro Braga, Thomas Burkhart and Bernd Lauke. "Viscoelastic behavior of multiwalled carbon nanotubes into phenolic resin." *Materials Research* 16 (2013): 713-720. <https://doi.org/10.1590/S1516-14392013005000045>
- [19] Çoban Kayıkçı, Fatma and Reşat Köşker. "Stability analysis of double-walled and triple-walled carbon nanotubes having local curvature." *Archive of Applied Mechanics* 91, no. 4 (2021): 1669-1681. <https://doi.org/10.1007/s00419-020-01846-5>
- [20] Çoban Kayıkçı, Fatma and Reşat Köşker. "Stress distribution in an elastic body with a locally curved double-walled carbon nanotube." *Journal of the Brazilian Society of Mechanical Sciences and Engineering* 43, no. 1 (2021): 52. <https://doi.org/10.1007/s40430-020-02732-5>
- [21] Suhr, Jonghwan, Nikhil Koratkar, Pawel Koblinski and Pulickel Ajayan. "Viscoelasticity in carbon nanotube composites." *Nature materials* 4, no. 2 (2005): 134-137. <https://doi.org/10.1038/nmat1293>
- [22] Li, Mingyuan, Qiliang Wu and Bin Bai. "Size-dependent mechanics of viscoelastic carbon nanotubes: modeling, theoretical and numerical analysis." *Results in Physics* 19 (2020): 103383. <https://doi.org/10.1016/j.rinp.2020.103383>
- [23] Akbarov, Surkay D. "Microbuckling of a doublewalled carbon nanotube embedded in an elastic matrix." *International journal of Solids and Structures* 50, no. 16-17 (2013): 2584-2596. <https://doi.org/10.1016/j.ijsolstr.2013.04.010>
- [24] Akbarov, S. D. and S. Karakaya. "3D analyses of the global stability loss of the circular hollow cylinder made from viscoelastic composite material." *European Journal of Mechanics-A/Solids* 33 (2012): 48-66. <https://doi.org/10.1016/j.euromechsol.2011.11.005>
- [25] Babich, I. Yu, A. N. Guz and Vik N. Chekhov. "The three-dimensional theory of stability of fibrous and laminated materials." *International applied mechanics* 37, no. 9 (2001): 1103-1141. <https://doi.org/10.1023/A:1013299014155>
- [26] Hoff, Nicholas John. "Forty-first Wilbur Wright memorial lecture: buckling and stability." *The Aeronautical Journal* 58, no. 517 (1954): 3-52. <https://doi.org/10.1017/S0368393100098114>
- [27] Akbarov, S. D., T. Sisman and Nazmiye Yahnioglu. "On the fracture of the unidirectional composites in compression." *International journal of engineering science* 35, no. 12-13 (1997): 1115-1136. [https://doi.org/10.1016/S0020-7225\(97\)00020-7](https://doi.org/10.1016/S0020-7225(97)00020-7)
- [28] Akbarov, S. D. and Reşat Kosker. "Fiber buckling in a viscoelastic matrix." *Mechanics of composite materials* 37 (2001): 299-306. <https://doi.org/10.1023/A:1012388602610>
- [29] Akbarov, S. D. and S. Karakaya. "3D Analyses of the symmetric local stability loss of the circular hollow cylinder made from viscoelastic composite material." *Applied Mathematical Modelling* 36, no. 9 (2012): 4241-4260. <https://doi.org/10.1016/j.apm.2011.11.054>
- [30] Akbarov, Surkhay D., Kosker, Reşat and Fatma Çoban. "Theoretical Limit of Fracture of Composites Containing Unidirectional Low-Density Hollow Fibers with Local Curvature under Compression." *In Proc. Conf. on XVIII. National Mechanic Congress, Manisa*, (2013): 10-20.
- [31] Akbarov, Surkay and A. N. Guz. *Mechanics of Curved Composites*. Vol. 78. Springer Science & Business Media, 2000. <https://doi.org/10.1007/978-94-010-9504-4>
- [32] Babich, I. Yu and A. N. Guz'. "Stability of fibrous composites." (1992): 61-80. <https://doi.org/10.1115/1.3119749>
- [33] Kosker, Resat. "On internal stability loss of a row unidirected periodically located fibers in the visco-elastic matrix." *Thermal Science* 23, no. Suppl. 1 (2019): 427-438. <https://doi.org/10.2298/TSCI181128055K>
- [34] Guz, Aleksandr Nikolaevich. *Fundamentals of the three-dimensional theory of stability of deformable bodies*. Springer Science & Business Media, 2013.
- [35] Akbarov, Surkay D. *Stability loss and Buckling delamination*. Springer, Berlin, 2012. <https://doi.org/10.1007/978-3-642-30290-9>
- [36] Akbarov, S. D., R. Kosker and K. Simsek. "On the theoretical strength limit in compression of viscoelastic unidirectional fibrous composite materials." *In Proc. 7th Int. Fracture Conf.(October 19–21, 2005)*, vol. 2, pp. 791-800. 2005.